Improved reconstruction of nonlinear spatial encoding techniques with explicit intra-voxel dephasing

Kelvin Layton[1], Stefan Kroboth[1], Feng Jia[1], Sebastian Littin[1], Huijun Yu[1], and Maxim Zaitsev[1]
[1]*Medical Physics, University Medical Center Freiburg, Freiburg, Baden-Württemberg, Germany*

TARGET AUDIENCE Researchers with an interest in image reconstruction and novel encoding techniques.

PURPOSE The use of spatial encoding magnetic fields (SEMs) that vary nonlinearly over the field-of-view have great potential for imaging but also present new challenges[1]. The spatially varying resolution inherent to these encoding fields has been exploited for acquisition acceleration[1,2] region-specific image encoding[3] and reduced FOV imaging[4]. Nonlinear SEMs also present unique intra-voxel dephasing characteristics, previously explored in the slice direction[5]. In this work, we examine dephasing in the imaging plane and propose an accurate model for image reconstruction.

THEORY The signal of the l^{th} channel for encoding with arbitrary SEMs is given in Eq. (1),

$$s_l(t_i) = \int m(\boldsymbol{x}) c_l(\boldsymbol{x}) e^{j\boldsymbol{k}^T(t_i)\boldsymbol{\psi}(\boldsymbol{x})} d\boldsymbol{x} \qquad (1) \qquad m(\boldsymbol{x}) = \sum_p m_p \text{rect}\left(\frac{\boldsymbol{x}-\boldsymbol{x}_p}{W}\right) \qquad (2)$$

where m is the magnetization, c_l is the coil sensitivity of the l^{th} receive channel, $\boldsymbol{k}$ is a vector of encoding moments and $\boldsymbol{\psi}$ are the SEM fields. It is necessary to discretize the integral in Eq. (1) to perform image reconstruction. This is traditionally performed by assuming a voxel basis of delta distributions. Here, we adopt 'box' functions, with pixel width W, to explicitly model intra-voxel dephasing (Eq. (2)). We make two assumptions in order to compute the integral in Eq. (1). First, the arbitrary SEMs are approximately linear over the scale of a single voxel, i.e. $\boldsymbol{\psi}(\boldsymbol{x}) \approx \boldsymbol{\psi}(\boldsymbol{x}_p) + G_p(\boldsymbol{x}-\boldsymbol{x}_p)$, where G_p is the Jacobian of $\boldsymbol{\psi}$ evaluated at pixel location $\boldsymbol{x}_p$. Secondly, we assume the coil sensitivities are constant over a voxel. Both assumptions are reasonable for typical imaging resolutions. The signal equation reduces to separate integrals representing the Fourier transform of a box function in each spatial dimension, which yields,

$$s_l(t_i) = \sum_p m_p c_l(\boldsymbol{x}_p)\, \text{sinc}\left(W\boldsymbol{k}^T(t_i)\boldsymbol{g}_{p,x}\right) \text{sinc}\left(W\boldsymbol{k}^T(t_i)\boldsymbol{g}_{p,y}\right) e^{j\boldsymbol{k}^T(t_i)\boldsymbol{\psi}(\boldsymbol{x}_p)} \qquad (4)$$

where $\boldsymbol{g}_{p,x}$ and $\boldsymbol{g}_{p,y}$ are the first and second columns of G_p, respectively. The sinc function weighting in Eq. (4) supports the intuition that intra-voxel dephasing reduces the signal for large local gradients or large trajectory moments.

METHODS *Simulations*: Signal from three different voxels was simulated with 10^6 spins for the quadrupolar field in Fig. 1 (inset). The signal was calculated for increasing encoding moment using Eq. (4) and by averaging the simulated spins. *Experiments*: Data was obtained on a modified 3T scanner (Siemens, Erlangen, Germany) with a nonlinear gradient insert (Resonance Research Inc, Billerica, USA) to provide simultaneous control of five encoding fields, after slice selection. A single slice from cylindrical phantom filled with thin Plexiglas tubes was measured with a five-dimensional variance optimized trajectory[6]. Images were reconstructed with a conjugate gradient (CG) algorithm implemented on a GPU using the traditional signal model assuming delta voxel bases and the proposed model in Eq. (4). The variance of the pixels in the object and background regions were calculated at each iteration of the reconstruction.

RESULTS Fig. 1 displays the signal from the three voxels depicted in the inset. The theory and numerical simulations are in good agreement, with a normalized error less than 0.2%. As expected, the signal decreases for an increasing encoding moment. Furthermore, pixels experiencing a higher local gradient also exhibit reduced signal. Fig. 2 compares images from the same experimental data reconstructed with 20 CG iterations using delta voxel functions and the proposed model. The image from the proposed model exhibits less noise over the entire field-of-view. To quantify the improvement, the variance of pixels was calculated within background and object masks for each CG iteration, as shown in Fig. 3. The noise in both regions is reduced for the proposed model; equivalently, more CG iterations can be executed for the same noise amplification, demonstrating the proposed model is more consistent with the experimental data.

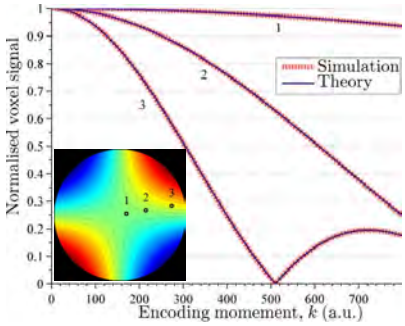

Fig. 1 Intra-voxel dephasing for three pixels encoded with a nonlinear field (inset) for increasing moment.

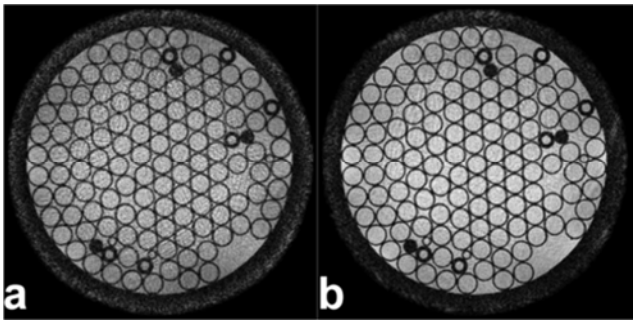

Fig. 2 Reconstructed images after 20 iterations of conjugate gradient using (a) the traditional signal model and (b) the proposed model incorporating intra-voxel dephasing.

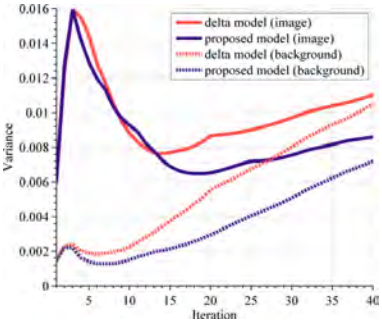

Fig. 3 Pixel variance over object and background regions for CG iterations using the traditional and proposed models.

CONCLUSION The reduction in signal from intra-voxel dephasing is as expected; however, the effect on image reconstruction is pronounced, particularly for nonlinear encoding strategies that push the limits of resolution. A model incorporating intra-voxel dephasing is more consistent with experiment data and consequently leads to superior images. Numerically integrating the encoding matrix or reconstructing at higher resolutions[7] can somewhat alleviate the inconsistency but is less accurate and requires substantially more computation than the presented model. Additionally, the model explicitly accounting for intra-voxel dephasing may be advantageous for imaging with traditional linear gradients.

REFERENCES [1]Schultz et al. 2010 MRM 64:1390–1403 [2]Stockmann et al. 2010 MRM 64:447–456 [3]Layton et al. 2013 MRM 70:684–696 [4]Witschey et al. 2012 MRM 67: 1620–1632 [5]Galiana et al. 2012 MRM 67:1120–1126 [6]Layton et al. Proc. ISMRM 2014 #32 [7]Stockmann et al. 2013 MRM 69:444–455

ACKNOWLEDGEMENTS This work was in part supported by European Research Council (ERC) grant 282345 'RANGEmri'